

This copy is for your personal, non-commercial use only.

If you wish to distribute this article to others, you can order high-quality copies for your colleagues, clients, or customers by [clicking here](#).

Permission to republish or repurpose articles or portions of articles can be obtained by following the guidelines [here](#).

The following resources related to this article are available online at www.sciencemag.org (this information is current as of July 29, 2011):

Updated information and services, including high-resolution figures, can be found in the online version of this article at:

<http://www.sciencemag.org/content/329/5987/75.full.html>

Supporting Online Material can be found at:

<http://www.sciencemag.org/content/suppl/2010/06/29/329.5987.75.DC1.html>

A list of selected additional articles on the Science Web sites **related to this article** can be found at:

<http://www.sciencemag.org/content/329/5987/75.full.html#related>

This article **cites 25 articles**, 9 of which can be accessed free:

<http://www.sciencemag.org/content/329/5987/75.full.html#ref-list-1>

This article has been **cited by** 19 articles hosted by HighWire Press; see:

<http://www.sciencemag.org/content/329/5987/75.full.html#related-urls>

This article appears in the following **subject collections**:

Genetics

<http://www.sciencemag.org/cgi/collection/genetics>

Digestive and Kidney Diseases) and The University of Luxembourg–Institute for Systems Biology Program to C.D.H. T.S.S. was supported by NIH Genetics Training Grant T32. All studies have been performed with informed consent approved by the Institutional Board of Qinghai Medical College of Qinghai University in Xining, Qinghai Province, People's Republic of China. All SNP genotypes are deposited in Gene Expression

Omnibus, with accession code GSE21661. These data, as well as phenotype data, are also available on our laboratory Web site, <http://forde-lab.genetics.utah.edu>. Please contact R.L.G. for access to DNA samples.

Supporting Online Material

www.sciencemag.org/cgi/content/full/science.1189406/DC1
Materials and Methods

Figs. S1 to S6
Tables S1 to S12
References

10 March 2010; accepted 6 May 2010
Published online 13 May 2010;
10.1126/science.1189406
Include this information when citing this paper.

Sequencing of 50 Human Exomes Reveals Adaptation to High Altitude

Xin Yi,^{1,2*} Yu Liang,^{1,2*} Emilia Huerta-Sanchez,^{3*} Xin Jin,^{1,4*} Zha Xi Ping Cuo,^{2,5*} John E. Pool,^{3,6*} Xun Xu,¹ Hui Jiang,¹ Nicolas Vinckenbosch,³ Thorfinn Sand Korneliusen,⁷ Hancheng Zheng,^{1,4} Tao Liu,¹ Weiming He,^{1,8} Kui Li,^{2,5} Ruibang Luo,^{1,4} Xifang Nie,¹ Honglong Wu,^{1,9} Meiru Zhao,¹ Hongzhi Cao,^{1,9} Jing Zou,¹ Ying Shan,^{1,4} Shuzheng Li,¹ Qi Yang,¹ Asan,^{1,2} Peixiang Ni,¹ Geng Tian,^{1,2} Junming Xu,¹ Xiao Liu,¹ Tao Jiang,^{1,9} Renhua Wu,¹ Guangyu Zhou,¹ Meifang Tang,¹ Junjie Qin,¹ Tong Wang,¹ Shuijian Feng,¹ Guohong Li,¹ Huasang,¹ Jiangbai Luosang,¹ Wei Wang,¹ Fang Chen,¹ Yading Wang,¹ Xiaoguang Zheng,^{1,2} Zhuo Li,¹ Zhuoma Bianba,¹⁰ Ge Yang,¹⁰ Xinpeng Wang,¹¹ Shuhui Tang,¹¹ Guoyi Gao,¹² Yong Chen,⁵ Zhen Luo,⁵ Lamu Gusang,⁵ Zheng Cao,¹ Qinghui Zhang,¹ Weihai Ouyang,¹ Xiaoli Ren,¹ Huiqing Liang,¹ Huisong Zheng,¹ Yebo Huang,¹ Jingxiang Li,¹ Lars Bolund,¹ Karsten Kristiansen,^{1,7} Yingrui Li,¹ Yong Zhang,¹ Xiuqing Zhang,¹ Ruiqiang Li,^{1,7} Songgang Li,¹ Huanming Yang,^{1,3,7†} Rasmus Nielsen,^{1,3,7†} Jun Wang,^{1,7†} Jian Wang^{1†}

Residents of the Tibetan Plateau show heritable adaptations to extreme altitude. We sequenced 50 exomes of ethnic Tibetans, encompassing coding sequences of 92% of human genes, with an average coverage of 18× per individual. Genes showing population-specific allele frequency changes, which represent strong candidates for altitude adaptation, were identified. The strongest signal of natural selection came from endothelial Per-Arnt-Sim (PAS) domain protein 1 (*EPAS1*), a transcription factor involved in response to hypoxia. One single-nucleotide polymorphism (SNP) at *EPAS1* shows a 78% frequency difference between Tibetan and Han samples, representing the fastest allele frequency change observed at any human gene to date. This SNP's association with erythrocyte abundance supports the role of *EPAS1* in adaptation to hypoxia. Thus, a population genomics survey has revealed a functionally important locus in genetic adaptation to high altitude.

The expansion of humans into a vast range of environments may have involved both cultural and genetic adaptation. Among the most severe environmental challenges to confront human populations is the low oxygen availability of high-altitude regions such as the Tibetan Plateau. Many residents of this region

live at elevations exceeding 4000 m, experiencing oxygen concentrations that are about 40% lower than those at sea level. Ethnic Tibetans possess heritable adaptations to their hypoxic environment, as indicated by birth weight (1), hemoglobin levels (2), and oxygen saturation of blood in infants (3) and adults after exercise (4). These results imply a history of natural selection for altitude adaptation, which may be detectable from a scan of genetic diversity across the genome.

We sequenced the exomes of 50 unrelated individuals from two villages in the Tibet Autonomous Region of China, both at least 4300 m in altitude (5). Exonic sequences were enriched with the NimbleGen (Madison, WI) 2.1M exon capture array (6), targeting 34 Mb of sequence from exons and flanking regions in nearly 20,000 genes. Sequencing was performed with the Illumina (San Diego, CA) Genome Analyzer II platform, and reads were aligned by using SOAP (7) to the reference human genome [National Center for Biotechnology Information (NCBI) Build 36.3].

Exomes were sequenced to a mean depth of 18× (table S1), which does not guarantee confident inference of individual genotypes. Therefore, we statistically estimated the probability of each possible genotype with a Bayesian algorithm (5) that

also estimated single-nucleotide polymorphism (SNP) probabilities and population allele frequencies for each site. A total of 151,825 SNPs were inferred to have >50% probability of being variable within the Tibetan sample, and 101,668 had >99% SNP probability (table S2). Sanger sequencing validated 53 of 56 SNPs that had at least 95% SNP probability and minor allele frequencies between 3% and 50%. Allele frequency estimates showed an excess of low-frequency variants (fig. S1), particularly for nonsynonymous SNPs.

The exome data was compared with 40 genomes from ethnic Han individuals from Beijing [the HapMap CHB sample, part of the 1000 genomes project (<http://1000genomes.org>)], sequenced to about fourfold coverage per individual. Beijing's altitude is less than 50 m above sea level, and nearly all Han come from altitudes below 2000 m. The Han sample represents an appropriate comparison for the Tibetan sample on the basis of low genetic differentiation between these samples ($F_{ST} = 0.026$). The two Tibetan villages show minimal evidence of genetic structure ($F_{ST} = 0.014$), and we therefore treated them as one population for most analyses. We observed a strong covariance between Han and Tibetan allele frequencies (Fig. 1) but with an excess of SNPs at low frequency in the Han and moderate frequency in the Tibetans.

Population historical models were estimated (8) from the two-dimensional frequency spectrum of synonymous sites in the two populations. The best-fitting model suggested that the Tibetan and Han populations diverged 2750 years ago, with the Han population growing from a small initial size and the Tibetan population contracting from a large initial size (fig. S2). Migration was inferred from the Tibetan to the Han sample, with recent admixture in the opposite direction.

Genes with strong frequency differences between populations are potential targets of natural selection. However, a simple ranking of F_{ST} values would not reveal which population was affected by selection. Therefore, we estimated population-specific allele frequency change by including a third, more distantly related population. We thus examined exome sequences from 200 Danish individuals, collected and analyzed as described for the Tibetan sample. By comparing the three pairwise F_{ST} values between these three samples, we can estimate the frequency change that occurred in the Tibetan population since its divergence from the Han population (5, 9). We found that this population branch statistic (PBS) has strong power to detect recent natural selection (fig. S3).

Genes showing extreme Tibetan PBS values represent strong candidates for the genetic basis

¹BGI-Shenzhen, Shenzhen 518083, China. ²The Graduate University of Chinese Academy of Sciences, Beijing 100062, China. ³Department of Integrative Biology and Department of Statistics, University of California Berkeley, Berkeley, CA 94820, USA. ⁴Innovative Program for Undergraduate Students, School of Bioscience and Biotechnology, South China University of Technology, Guangzhou 510641, China. ⁵The People's Hospital of the Tibet Autonomous Region, Lhasa 850000, China. ⁶Department of Evolution and Ecology, University of California Davis, Davis, CA 95616, USA. ⁷Department of Biology, University of Copenhagen, DK-1165 Copenhagen, Denmark. ⁸Innovative Program for Undergraduate Students, School of Science, South China University of Technology, Guangzhou 510641, China. ⁹Genome Research Institute, Shenzhen University Medical School, Shenzhen 518060, China. ¹⁰The People's Hospital of Lhasa, Lhasa, 850000, China. ¹¹The Military General Hospital of Tibet, Lhasa, 850007, China. ¹²The Hospital of XiShuangBanNa Dai Nationalities, Autonomous Jinghong 666100, Yunnan, China.

*These authors contributed equally to this work.
†To whom correspondence should be addressed. E-mail: wangjian@genomics.org.cn (J.W.); wangj@genomics.org.cn (J.W.); rasmus_nielsen@berkeley.edu (R.N.)

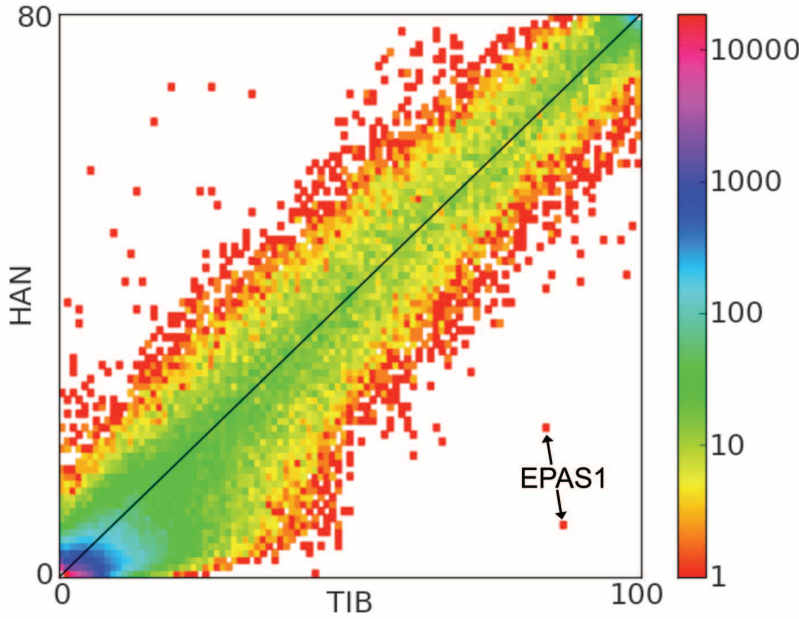


Fig. 1. Two-dimensional unfolded site frequency spectrum for SNPs in Tibetan (x axis) and Han (y axis) population samples. The number of SNPs detected is color-coded according to the logarithmic scale plotted on the right. Arrows indicate a pair of intronic SNPs from the *EPAS1* gene that show strongly elevated derived allele frequencies in the Tibetan sample compared with the Han sample.

Table 1. Genes with strongest frequency changes in the Tibetan population. The top 30 PBS values for the Tibetan branch are listed. Oxygen-related candidate genes within 100 kb of these loci are noted. For FXYD, F indicates Phe; Y, Tyr; D, Asp; and X, any amino acid.

Gene	Description	Nearby candidate	PBS	P value
<i>EPAS1</i>	Endothelial PAS domain protein 1 (HIF-2 α)	(Self)	0.514	<0.000001
<i>C1orf124</i>	Hypothetical protein LOC83932	<i>EGLN1</i>	0.277	0.000203
<i>DISC1</i>	Disrupted in schizophrenia 1	<i>EGLN1</i>	0.251	0.000219
<i>ATP6V1E2</i>	Adenosine triphosphatase (ATPase), H+ transporting, lysosomal 31 kD, V1	<i>EPAS1</i>	0.246	0.000705
<i>SPP1</i>	Secreted phosphoprotein 1		0.238	0.000562
<i>PKLR</i>	Pyruvate kinase, liver, and RBC	(Self)	0.230	0.000896
<i>C4orf7</i>	Chromosome 4 open reading frame 7		0.227	0.001098
<i>PSME2</i>	Proteasome activator subunit 2		0.222	0.001103
<i>OR10X1</i>	Olfactory receptor, family 10, subfamily X	<i>SPTA1</i>	0.218	0.000950
<i>FAM9C</i>	Family with sequence similarity 9, member C	<i>TMSB4X</i>	0.216	0.001389
<i>LRRC3B</i>	Leucine-rich repeat-containing 3B		0.215	0.001405
<i>KRTAP21-2</i>	Keratin-associated protein 21-2		0.213	0.001470
<i>HIST1H2BE</i>	Histone cluster 1, H2be	<i>HFE</i>	0.212	0.001568
<i>TTL3</i>	Tubulin tyrosine ligase-like family, member 3		0.206	0.001146
<i>HIST1H4B</i>	Histone cluster 1, H4b	<i>HFE</i>	0.204	0.001404
<i>ACVR1B</i>	Activin A type IB receptor isoform a precursor	<i>ACVRL1</i>	0.198	0.002041
<i>FXYD6</i>	FXYD domain-containing ion transport regulator		0.192	0.002459
<i>NAGLU</i>	Alpha-N-acetylglucosaminidase precursor		0.186	0.002834
<i>MDH1B</i>	Malate dehydrogenase 1B, nicotinamide adenine dinucleotide (NAD) (soluble)		0.184	0.002113
<i>OR6Y1</i>	Olfactory receptor, family 6, subfamily Y	<i>SPTA1</i>	0.183	0.002835
<i>HBB</i>	Beta globin	(Self), <i>HBG2</i>	0.182	0.003128
<i>OTX1</i>	Orthodenticle homeobox 1		0.181	0.003235
<i>MBNL1</i>	Muscleblind-like 1		0.179	0.002410
<i>IFI27L1</i>	Interferon, alpha-inducible protein 27-like 1		0.179	0.003064
<i>C18orf55</i>	Hypothetical protein LOC29090		0.178	0.002271
<i>RFX3</i>	Regulatory factor X3		0.176	0.002632
<i>HBG2</i>	G-gamma globin	(Self), <i>HBB</i>	0.170	0.004147
<i>FANCA</i>	Fanconi anemia, complementation group A	(Self)	0.169	0.000995
<i>HIST1H3C</i>	Histone cluster 1, H3c	<i>HFE</i>	0.168	0.004287
<i>TMEM206</i>	Transmembrane protein 206		0.166	0.004537

of altitude adaptation. The strongest such signals include several genes with known roles in oxygen transport and regulation (Table 1 and table S3). Overall, the 34 genes in our data set that fell under the gene ontology category “response to hypoxia” had significantly greater PBS values than the genome-wide average ($P = 0.00796$).

The strongest signal of selection came from the endothelial Per-Arnt-Sim (PAS) domain protein 1 (*EPAS1*) gene. On the basis of frequency differences among the Danes, Han, and Tibetans, *EPAS1* was inferred to have a very long Tibetan branch relative to other genes in the genome (Fig. 2). In order to confirm the action of natural selection, PBS values were compared against neutral simulations under our estimated demographic model. None of one million simulations surpassed the PBS value observed for *EPAS1*, and this result remained statistically significant after accounting for the number of genes tested ($P < 0.02$ after Bonferroni correction). Many other genes had uncorrected P values below 0.005 (Table 1), and, although none of these were statistically significant after correcting for multiple tests, the functional enrichment suggests that some of these genes may also contribute to altitude adaptation.

EPAS1 is also known as hypoxia-inducible factor 2 α (*HIF-2 α*). The HIF family of transcription factors consist of two subunits, with three

alternate α subunits (*HIF-1 α* , *HIF-2 α* /*EPAS1*, *HIF-3 α*) that dimerize with a β subunit encoded by *ARNT* or *ARNT2*. *HIF-1 α* and *EPAS1* each act on a unique set of regulatory targets (10), and the narrower expression profile of *EPAS1* includes adult and fetal lung, placenta, and vascular endothelial cells (11). A protein-stabilizing mutation in *EPAS1* is associated with erythrocytosis (12), suggesting a link between *EPAS1* and the regulation of red blood cell production.

Although our sequencing primarily targeted exons, some flanking intronic and untranslated region (UTR) sequence was included. The *EPAS1* SNP with the greatest Tibetan-Han frequency difference was intronic (with a derived allele at 9% frequency in the Han and 87% in the Tibetan sample; table S4), whereas no amino acid-changing variant had a population frequency difference of greater than 6%. Selection may have acted directly on this variant, or another linked noncoding variant, to influence the regulation of *EPAS1*. Detailed molecular studies will be needed to investigate the direction and the magnitude of gene expression changes associated with this SNP, the tissues and developmental time points affected, and the downstream target genes that show altered regulation.

Associations between SNPs at *EPAS1* and athletic performance have been demonstrated (13). Our data set contains a different set of SNPs, and we conducted association testing on the SNP with the most extreme frequency difference, located just upstream of the sixth exon. Alleles at this SNP tested for association with blood-related phenotypes showed no relationship with oxygen saturation. However, significant associations were discovered for erythrocyte count (F test $P = 0.00141$) and for hemoglobin concentration (F test $P = 0.00131$), with significant or marginally significant P values for both traits when each

village was tested separately (table S5). Comparison of the *EPAS1* SNP to genotype data from 48 unlinked SNPs confirmed that its P value is a strong outlier (5) (fig. S4).

The allele at high frequency in the Tibetan sample was associated with lower erythrocyte quantities and correspondingly lower hemoglobin levels (table S4). Because elevated erythrocyte production is a common response to hypoxic stress, it may be that carriers of the “Tibetan” allele of *EPAS1* are able to maintain sufficient oxygenation of tissues at high altitude without the need for increased erythrocyte levels. Thus, the hematological differences observed here may not represent the phenotypic target of selection and could instead reflect a side effect of *EPAS1*-mediated adaptation to hypoxic conditions. Although the precise physiological mechanism remains to be discovered, our results suggest that the allele targeted by selection is likely to confer a functionally relevant adaptation to the hypoxic environment of high altitude.

We also identified components of adult and fetal hemoglobin (*HBB* and *HBB2*, respectively) as putatively under selection. These genes are located only ~20 kb apart (fig. S5), so their PBS values could reflect a single adaptive event. For both genes, the SNP with the strongest Tibetan-Han frequency difference is intronic. Although altered globin proteins have been found in some altitude-adapted species (14), in this case regulatory changes appear more likely. A parallel result was reported in Andean highlanders, with promoter variants at *HBB2* varying with altitude and associated with a delayed transition from fetal to adult hemoglobin (15).

Aside from *HBB*, two other anemia-associated genes were identified: *FANCA* and *PKLR*, associated with erythrocyte production and maintenance, respectively (16, 17). We also identified

genes associated with diseases linked to low oxygen during pregnancy or birth: schizophrenia (*DISC1* and *FXYD6*) (18, 19) and epilepsy (*OTX1*) (20). However, the strong signal of selection affecting *DISC1*, along with *C1orf124*, might instead trace to a regulatory region of *EGLN1*, which lies between these loci (fig. S5) and functions in the hypoxia response pathway (21).

Other genes identified in this study are also located near candidate genes. *OR10X1* and *OR6Y1* are within ~60 kb of the *SPTA1* gene (fig. S5), which is associated with erythrocyte shape (22). Additionally, the three histones implicated in this study (Table 1) are clustered around *HFE* (fig. S5), a gene involved in iron storage (23). The influence of population genetic signals on neighboring genes is consistent with recent and strong selection imposed by the hypoxic environment. Stronger frequency changes at flanking genes might be expected if adaptive mutations have targeted candidate gene regulatory regions that are not near common exonic polymorphisms.

Of the genes identified here, only *EGLN1* was mentioned in a recent SNP variation study in Andean highlanders (24). This result is consistent with the physiological differences observed between Tibetan and Andean populations (25), suggesting that these populations have taken largely distinct evolutionary paths in altitude adaptation.

Several loci previously studied in Himalayan populations showed no signs of selection in our data set (table S6), whereas *EPAS1* has not been a focus of previous altitude research. Although *EPAS1* may play an important role in the oxygen regulation pathway, this gene was identified on the basis of a noncandidate population genomic survey for natural selection, illustrating the utility of evolutionary inference in revealing functionally important loci.

Given our estimate that Han and Tibetans diverged 2750 years ago and experienced subsequent migration, it appears that our focal SNP at *EPAS1* may have experienced a faster rate of frequency change than even the lactase persistence allele in northern Europe, which rose in frequency over the course of about 7500 years (26). *EPAS1* may therefore represent the strongest instance of natural selection documented in a human population, and variation at this gene appears to have had important consequences for human survival and/or reproduction in the Tibetan region.

References and Notes

1. L. G. Moore, *High Alt. Med. Biol.* **2**, 257 (2001).
2. T. Wu *et al.*, *J. Appl. Physiol.* **98**, 598 (2005).
3. S. Niermeyer *et al.*, *N. Engl. J. Med.* **333**, 1248 (1995).
4. J. Zhuang *et al.*, *Respir. Physiol.* **103**, 75 (1996).
5. Materials and methods are available as supporting material on Science Online.
6. T. J. Albert *et al.*, *Nat. Methods* **4**, 903 (2007).
7. R. Li *et al.*, *Bioinformatics* **25**, 1966 (2009).
8. R. N. Gutenkunst, R. D. Hernandez, S. H. Williamson, C. D. Bustamante, G. McVean, *PLoS Genet.* **5**, e1000695 (2008).
9. M. D. Shriver *et al.*, *Hum. Genomics* **1**, 274 (2004).
10. C.-J. Hu, L.-Y. Wang, L. A. Chodosh, B. Keith, M. C. Simon, *Mol. Cell. Biol.* **23**, 9361 (2003).

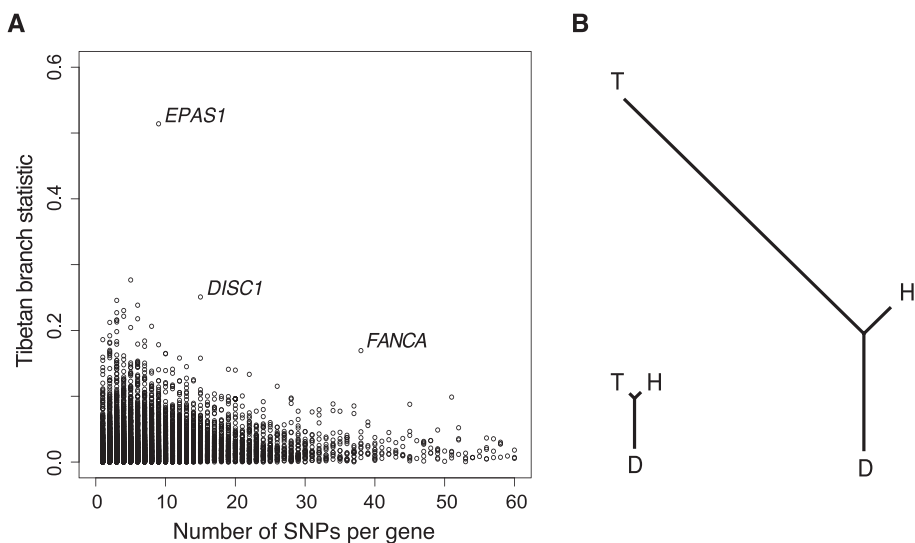


Fig. 2. Population-specific allele frequency change. (A) The distribution of F_{ST} -based PBS statistics for the Tibetan branches, according to the number of variable sites in each gene. Outlier genes are indicated in red. (B) The signal of selection on *EPAS1*: Genomic average F_{ST} -based branch lengths for Tibetan (T), Han (H), and Danish (D) branches (left) and branch lengths for *EPAS1*, indicating substantial differentiation along the Tibetan lineage (right).

11. S. Jain, E. Maltepe, M. M. Lu, C. Simon, C. A. Bradfield, *Mech. Dev.* **73**, 117 (1998).
12. M. J. Percy *et al.*, *N. Engl. J. Med.* **358**, 162 (2008).
13. J. Henderson *et al.*, *Hum. Genet.* **118**, 416 (2005).
14. J. F. Storz *et al.*, *Proc. Natl. Acad. Sci. U.S.A.* **106**, 14450 (2009).
15. I. Rottgardt, F. Rothhammer, M. Dittmar, *Anthropol. Sci.* **118**, 41 (2010).
16. H. Kanno, H. Fujii, A. Hirono, M. Omine, S. Miwa, *Blood* **79**, 1347 (1992).
17. X. Zhang, J. Li, D. P. Sejas, Q. Pang, *Blood* **106**, 75 (2005).
18. C. A. Hodgkinson *et al.*, *Am. J. Hum. Genet.* **75**, 862 (2004).
19. K. Choudhury *et al.*, *Am. J. Hum. Genet.* **80**, 664 (2007).
20. D. Acampora *et al.*, *Nat. Genet.* **14**, 218 (1996).
21. K. K. W. To, L. E. Huang, *J. Biol. Chem.* **280**, 38102 (2005).
22. M. Gaetani, S. Mootien, S. Harper, P. G. Gallagher, D. W. Speicher, *Blood* **111**, 5712 (2008).
23. M. W. Hentze, M. U. Muckenthaler, N. C. Andrews, *Cell* **117**, 285 (2004).
24. A. W. Bigham *et al.*, *Hum. Genomics* **4**, 79 (2009).
25. C. M. Beall, *Proc. Natl. Acad. Sci. U.S.A.* **104** (suppl. 1), 8655 (2007).
26. Y. Itan *et al.*, *PLOS Comput. Biol.* **5**, e1000491 (2009).
27. This research was funded by the National Natural Science Foundation of China (grants 30890032 and 30725008), the Ministry of Science and Technology of China (863 program, grants 2006AA02A302 and 2009AA022707; 973 program, grant 2006CB504103), the Shenzhen Municipal Government of China (grants JC200903190772A, CXB200903110066A, ZYC200903240077A, ZYC200903240076A, and ZYC200903240080A), the Ole Rømer grant from the Danish Natural Science Research Council, the Solexa project (272-07-0196), the Danish Strategic Research Council grant (2106-07-0021), the Lundbeck Foundation, the Swiss National Science Foundation (PBLAP3-124318), the U.S. NIH

(R01MHG084695 and R01HG003229), the U.S. NSF (DBI-0906065), the Chinese Academy of Sciences (KSCX2-YW-R-76), and the Science and Technology Plan of the Tibet Autonomous Region (no. 2007-2-18). We are also indebted to many additional faculty and staff of BGI-Shenzhen who contributed to this teamwork and to X. Wang (South China University of Technology). The data have NCBI Short Read Archive accession no. SRA012603.

Supporting Online Material

www.sciencemag.org/cgi/content/full/329/5987/75/DC1

Materials and Methods

Figs. S1 to S5

Tables S1 to S6

References

1 April 2010; accepted 21 May 2010

10.1126/science.1190371

Genome-Wide Reprogramming in the Mouse Germ Line Entails the Base Excision Repair Pathway

Petra Hajkova,^{1,3,*} Sean J. Jeffries,^{1,4,*} Caroline Lee,¹ Nigel Miller,² Stephen P. Jackson,^{1,5} M. Azim Surani^{1,†}

Genome-wide active DNA demethylation in primordial germ cells (PGCs), which reprograms the epigenome for totipotency, is linked to changes in nuclear architecture, loss of histone modifications, and widespread histone replacement. Here, we show that DNA demethylation in the mouse PGCs is mechanistically linked to the appearance of single-stranded DNA (ssDNA) breaks and the activation of the base excision repair (BER) pathway, as is the case in the zygote where the paternal pronucleus undergoes active DNA demethylation shortly after fertilization. Whereas BER might be triggered by deamination of a methylcytosine (5mC), cumulative evidence indicates other mechanisms in germ cells. We demonstrate that DNA repair through BER represents a core component of genome-wide DNA demethylation in vivo and provides a mechanistic link to the extensive chromatin remodeling in developing PGCs.

The specification of mouse primordial germ cells (PGCs) at embryonic day 7.25 (E7.25) is accompanied by the initiation of epigenetic changes (1), followed by widespread epigenetic reprogramming at E11.5, which includes genome-wide DNA demethylation, erasure of genomic imprints, and large-scale chromatin remodeling (1–3) (fig. S1). Chromatin remodeling follows the onset of genome-wide DNA demethylation, which suggests that DNA repair might be linked to this process (2). DNA repair–driven DNA demethylation would involve replacement

of a methylcytosine (5mC)–containing nucleotide by an unmethylated cytosine (4, 5). As the epigenetic changes in E11.5 PGCs occur in the G₂ phase of the cell cycle and are thus independent of DNA replication (2), the most likely mechanisms for the replacement of 5mC would be the nucleotide excision repair (NER) or base excision repair (BER) pathways.

We obtained a quantitative measure of expression of BER and NER components and observed an up-regulation of transcripts of BER components *Parp1*, *Ape1*, and *Xrcc1* in E11.5 PGCs, which was not seen in the neighboring somatic cells (6). By contrast, we observed little expression of NER components *Ercc1* and *Xpa* in these PGCs (Fig. 1A and fig. S2).

Expression of ERCC1 (excision repair cross-complementing rodent repair deficiency, complementation group 1), a core NER component, occurs at low levels in PGCs and neighboring somatic cells at the time of epigenetic reprogramming compared with control ultraviolet light–irradiated primary embryonic fibroblasts (PEFs), where we observed a dose-dependent increase and nuclear localization of ERCC1 (fig.

S3). Although we detected XPA—another NER component—in both somatic cells and PGCs (fig. S4A), it was not chromatin bound and, hence, was inactive (7) (fig. S4B). Thus, the response of the NER pathway is not triggered during the reprogramming process in PGCs.

XRCC1 (x-ray repair complementing defective repair in Chinese hamster cells 1), a core component of the BER pathway (8), is present in PGC nuclei between E10.5 and E12.5 (fig. S5A), as is PARP1 [poly(ADP-ribose) polymerase family, member 1] and APE1 (apurinic/apyrimidinic endonuclease) (fig. S5, B and C). XRCC1 is a soluble nuclear factor, which binds to DNA when single-stranded DNA (ssDNA) breaks occur (8). We determined the amount of chromatin-bound XRCC1 in gonadal PGCs using the preextraction method (9). Whereas we observed an overall enrichment of XRCC1 in PGCs during E10.5 to E12.5, we found an enhancement in chromatin-bound XRCC1, specifically in PGCs at E11.5, which coincides with the stage at which genome-wide DNA demethylation occurs (Fig. 1B), which suggested that ssDNA breaks are present (10). We also detected high levels of PAR polymer, a product of activated PARP1 enzyme and an additional marker of active BER (8, 11), specifically in E11.5 PGCs (Fig. 1C). The presence of activated BER in PGCs during ongoing epigenetic reprogramming suggests that DNA demethylation in PGCs may be linked to the DNA repair pathway (2).

In PGCs spanning a period of ~6 hours, between E11.25 and E11.5, we detected increasing levels of PAR before the loss of signal for histone H1 (Fig. 1C). Because histone H1 is a target for PARP1 ribosylation (11, 12) and PARP1 itself has been shown to displace H1 (13), it is possible that high levels of PARP1-mediated poly(ADP-ribose) (PAR) synthesis in the nuclei of PGCs might be involved in H1 displacement. Additionally, we observed a correlation between high nuclear PAR signals and the disappearance of chromocenters in PGCs (fig. S5D) (2), which is consistent with a proposed role for PARP1 in the regulation of higher-order chromatin structure (11, 14, 15).

¹Wellcome Trust–Cancer Research U.K. Gurdon Institute of Cancer and Developmental Biology, University of Cambridge, Tennis Court Road, Cambridge CB2 1QN, UK. ²Department of Pathology, University of Cambridge, Tennis Court Road, Cambridge CB2 1QP, UK. ³Medical Research Council Clinical Sciences Centre, Hammersmith Hospital Campus, Du Cane Road, London W12 0NN, UK. ⁴Templeman Automation, 21 Properzi Way, Somerville, MA 02143, USA. ⁵Department of Biochemistry, University of Cambridge, Cambridge CB2 1QW, UK.

*These authors contributed equally to this work.

†To whom correspondence should be addressed. E-mail: a.surani@gurdon.cam.ac.uk (M.A.S.), petra.hajkova@csc.mrc.ac.uk (P.H.)